

Muon-spin-rotation studies in single-crystal $\text{Sr}_2\text{CuO}_2\text{Cl}_2$

L. P. Le, G. M. Luke, B. J. Sternlieb, and Y. J. Uemura
Department of Physics, Columbia University, New York, New York 10027

J. H. Brewer and T. M. Riseman
Department of Physics, University of British Columbia, Vancouver, Canada V6T 2A3

D. C. Johnston and L. L. Miller
Ames Laboratory-United States Department of Energy and Department of Physics, Iowa State University, Ames, Iowa 50011
 (Received 5 April 1990)

We report zero-field muon-spin-rotation studies on single crystals of $\text{Sr}_2\text{CuO}_2\text{Cl}_2$ between 5 and 300 K. Magnetic order below the Néel temperature is observed, and the results are compared with those of neutron diffraction measurements. The temperature dependence of the muon precession frequencies exhibits properties characteristic to two-dimensional spin- $\frac{1}{2}$ systems with a dominant Heisenberg interaction and very small anisotropy. The splitting of the muon precession frequency below 60 K indicates either a magnetic phase transition or a change in the μ^+ site. By comparing the observed static internal field with the calculated dipolar field from Cu^{2+} moments in the crystal we found that the muon sites are located near the center of CuO_2 planes.

I. INTRODUCTION

Since the discovery of high- T_c superconductivity in $\text{La}_{1.85}\text{Ba}_{0.15}\text{CuO}_4$,¹ there has been considerable interest in layered CuO_2 materials. To date, all insulating parent compounds of the planar cuprate superconductor exhibit long-range antiferromagnetic order. $\text{Sr}_2\text{CuO}_2\text{Cl}_2$ is a layered perovskite with the body-centered-tetragonal ($I4/mmm$) K_2NiF_4 structure.^{2,3} Recent neutron diffraction and magnetic susceptibility studies⁴ have shown that $\text{Sr}_2\text{CuO}_2\text{Cl}_2$ orders magnetically, with a three-dimensional antiferromagnetic structure (spin $\frac{1}{2}$) similar to that found in La_2CuO_4 . As shown in Fig. 1(a) the structure contains CuO_2 planes, a common feature to all high- T_c cuprates. In $\text{Sr}_2\text{CuO}_2\text{Cl}_2$ however these layers are separated by puckered SrCl rocksalt layers, which leads the c -axis parameter to be 20% larger than in other cuprate compounds. Comparison with Nd_2CuO_4 [Fig. 1(c)], the parent compound of electron-doped superconductor ($\text{Nd}_{1-x}\text{Ce}_x$) $_2\text{CuO}_{4-y}$, shows that both systems lack apical oxygens. This effectively results in a net positive charge around the copper atoms and thus electrons may be attracted to these sites. The Madelung potentials for introducing an electron at copper sites⁵ in Nd_2CuO_4 and $\text{Sr}_2\text{CuO}_2\text{Cl}_2$ are much lower than in other cuprate materials, such as La_2CuO_4 . This similarity between Nd_2CuO_4 and $\text{Sr}_2\text{CuO}_2\text{Cl}_2$ suggests that $\text{Sr}_2\text{CuO}_2\text{Cl}_2$ is a candidate for electron doping. To date, however, there has been no success in creating a superconductor based on this system.

In La_2CuO_4 , an orthorhombic distortion contributes to the effective anisotropic exchange interaction between the spins on adjacent CuO_2 planes. The Néel temperature T_N of La_2CuO_4 is very sensitive to detailed stoichiometry of oxygen.^{6,7} In Nd_2CuO_4 , neutron⁸ and μ^+ SR (Ref. 9)

studies have revealed a successive spin reorientations at $T \sim 75$ and 35 K. With a larger separation between CuO_2 planes, $\text{Sr}_2\text{CuO}_2\text{Cl}_2$ provides a good example for investigating the two-dimensional spin- $\frac{1}{2}$ system.

In this paper we report muon spin rotation and relaxation studies of single crystals of $\text{Sr}_2\text{CuO}_2\text{Cl}_2$. The temperature dependence of the muon spin precession frequency indicates that the magnetic properties of this system show features characteristic to 2D spin- $\frac{1}{2}$ Heisenberg antiferromagnets with an additional very small anisotropy energy. In μ^+ SR, the determination of muon sites in a substance is important. The muon sites are studied by

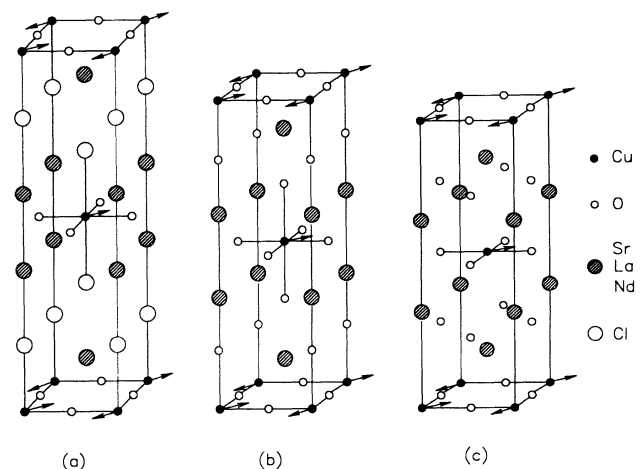


FIG. 1. Crystal structures of (a) $\text{Sr}_2\text{CuO}_2\text{Cl}_2$, (b) La_2CuO_4 , (c) Nd_2CuO_4 . The arrows on coppers indicate the spin direction. In Nd_2CuO_4 , two spin-flip transitions are at the centered copper.

comparing the observed local field at the muon site with calculation of dipolar fields from the Cu^{2+} moments. In La_2CuO_4 and Nd_2CuO_4 , the muon sites are likely near the out-of-plane oxygens. In $\text{Sr}_2\text{CuO}_2\text{Cl}_2$ we show that the muon sites are located around the center of the four oxygen atoms in the CuO_2 plane.

II. EXPERIMENTAL ASPECTS

The principle of the μ^+ SR technique has been described previously.¹⁰ In a zero-field μ^+ SR experiment, a beam of $\sim 100\%$ polarized muons is focused on a target sample. After stopping almost instantaneously at interstitial sites, each muon precesses in the internal field at a frequency $\nu = \gamma_\mu H_{\text{int}}$ ($\gamma_\mu = 13.554$ MHz/kG). When the muon decays, the decay positron is emitted preferentially along the muon spin direction. As a result, the accumulated positron time histograms allow one to monitor the muon spin evolution.

Figure 2 illustrates the experiment configuration. Single crystal specimens, each approximately $5 \times 5 \times 0.5$ mm³, were prepared as described in Ref. 2. The mosaic sample composed of several single crystals were mounted in a ⁴He gas flow cryostat with their *c* axis aligned parallel to the beam direction. We used the low energy (28 MeV/c) “surface muon” beam obtained at the *M15* and *M20* muon channels at TRIUMF (Vancouver). To investigate the direction of the internal field, the spin polarization of incident muons was rotated with a Wien filter either parallel or perpendicular to the *c* axis [configurations (a) and (b) in Fig. 2]. The positron detectors were placed forward/backward or upward/downward of the sample volume, with respect to the initial muon spin direction.

The number of positrons detected in the opposing counters (for example, *F* and *B* stand for forward and backward) is given by

$$N_F(t) = N_F^0 \exp(-t/\tau_\mu) [1 + A_F P(t)], \quad (1)$$

$$N_B(t) = N_B^0 \exp(-t/\tau_\mu) [1 - A_B P(t)], \quad (2)$$

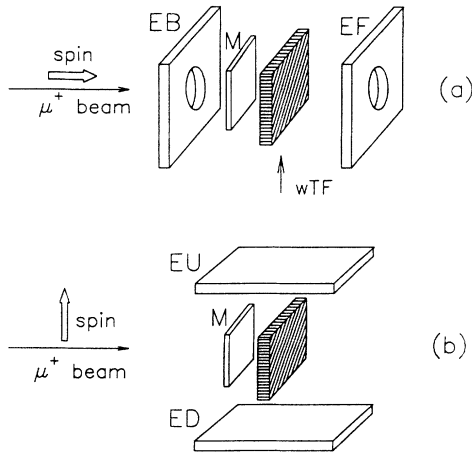


FIG. 2. Schematic view of the ZF- μ^+ SR experiment configuration. The polarized muon beam is identified by *M* and the decay positrons are detected by counters: (a) *EF* and *EB*, (b) *EU* and *ED*.

where N_F^0 and N_B^0 are the counting rates, $\tau_\mu = 2.2$ μs is muon lifetime, A_F and A_B denote the initial decay asymmetry (usually $A = 0.2 \sim 0.3$), $P(t)$ is the muon spin polarization as a function of the time t . Assuming $A_F \approx A_B$ we define the corrected asymmetry $\mathcal{A}(t)$ proportional to muon polarization $P(t)$ as

$$\mathcal{A}(t) = \frac{N_F(t) - \alpha N_B(t)}{N_F(t) + \alpha N_B(t)} = AP(t), \quad (3)$$

where $\alpha = N_F^0/N_B^0$ is a geometrical factor, generally $\alpha \sim 1$. Thus the spin evolution is deduced from positron histograms.

III. RESULTS

Figure 3 shows the time spectra of the muon polarization $\mathcal{A}(t)$ observed in $\text{Sr}_2\text{CuO}_2\text{Cl}_2$ in zero field at several temperatures. For both initial muon polarization directions, spin precession is clearly seen. Fourier transforms (Fig. 4) show that there are two high frequencies present at low temperature ($T < 60$ K), and one frequency between 60 and 250 K. Therefore, the μ^+ SR data are analyzed with the approximation

$$\mathcal{A}(t) = \sum_i^n A_i \exp(-\Delta_i t) \cos(\omega_i t + \phi) + A_{\text{non}} \exp(-\Delta_{\text{non}} t), \quad (4)$$

where A_i and A_{non} are the asymmetries of oscillating and nonoscillating components; $\omega_i/2\pi = \nu_i$ is the muon precession frequency; Δ_i and Δ_{non} are the relaxation rates; $n = 2$ for $T < 60$ K, and $n = 1$ for $T \geq 60$ K.

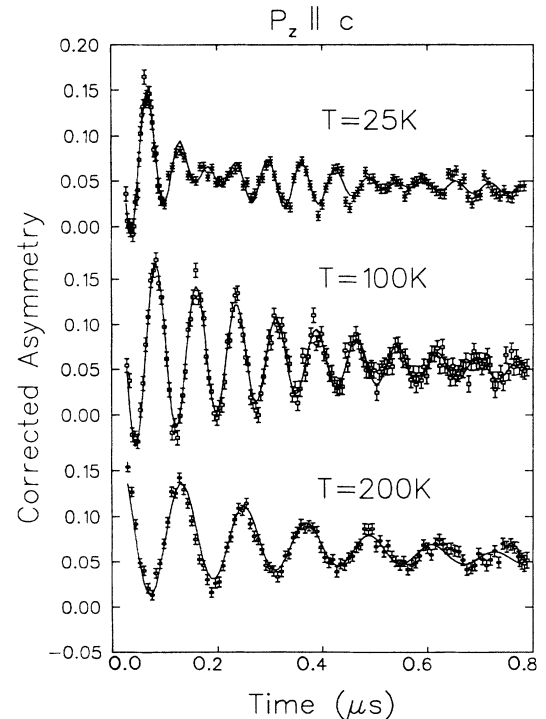


FIG. 3. Corrected asymmetry from counters *EF* and *EB*. The solid curve is from the fit of Eq. (4).

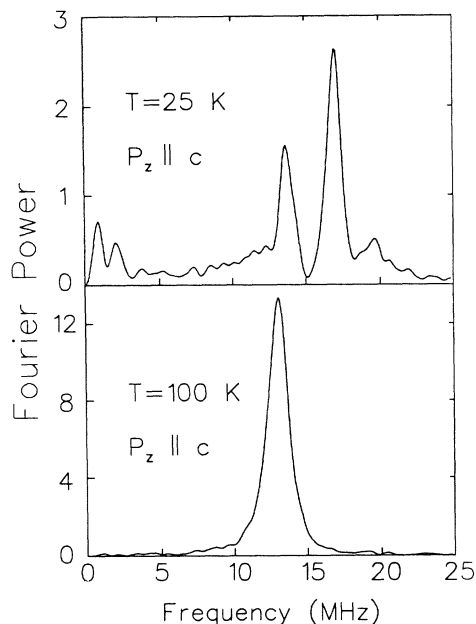


FIG. 4. Fourier power vs frequency.

Figure 5 illustrates the temperature dependence of the muon precession frequency. The frequency is sharply reduced above 250 K; the oscillating component totally disappears around 270 K. This is consistent with the neutron experiments⁴ which found $T_N \approx 250$ K on similar crystals. The disappearance of the oscillating signal¹¹ is due to the transition to the paramagnetic phase occurred at Néel temperature ($T_N = 260 \pm 10$ K). Below 250 K, long-lived oscillations in muon spin polarization are characteristic of static magnetic order.

At low temperatures ($T \rightarrow 0$ K), the precession frequency is centered around 16 MHz (equivalent to a field of 1.2 kG at muon site), which is much higher than that in $\text{La}_2\text{CuO}_{4-y}$ (Refs. 7 and 12) (~ 5 MHz). The curve

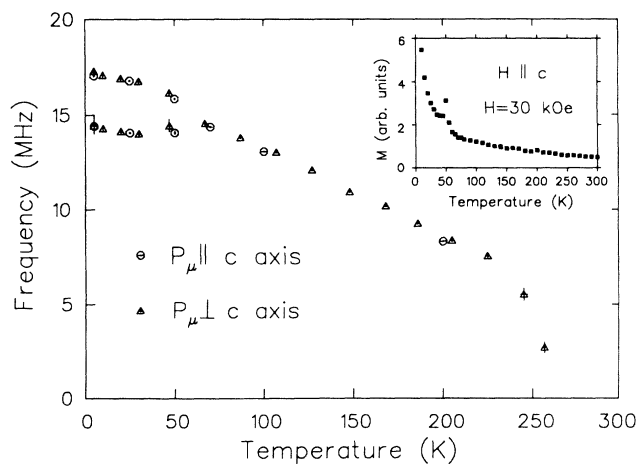


FIG. 5. Muon precession frequency vs temperature. A splitting is found around 60 K. Inserted in the upper-right corner is the temperature dependence of magnetization. A peak is found around 50 K.

splits into two lines below 60 K. This may be from either an intrinsic effect of possible spin reorientation in $\text{Sr}_2\text{CuO}_2\text{Cl}_2$ or alternatively the effect due to possible change of the muon sites at low temperatures. Neutron studies have not detected any structural transition from the tetragonal $I4/mmm$. However, our measurements on magnetic susceptibility (with an applied field $H = 3$ T as shown in the upper-right corner of Fig. 5) exhibit a peak present around 50 K. This peak is only observed when the field is parallel to the c axis, and exhibits hysteresis between field-cooled and zero-field-cooled measurements.⁴ This may suggest that the splitting is caused by some intrinsic changes in $\text{Sr}_2\text{CuO}_2\text{Cl}_2$ rather than by a muon site change.

Below T_N , roughly 60% of the μ^+ polarization is seen in the oscillating signal when $\mathbf{P}(0) \parallel c$ and 33% when $\mathbf{P}(0) \perp c$. The ratio of the polarizations is 1.8 ± 0.3 indicating that the internal field is essentially parallel to the ab plane. This can be explained as follows. Since the samples are tetragonal, there will be at least two magnetic domains in the sample. In addition, the equivalent a - b axes were not oriented. Therefore, on average, there is the same probability of finding the internal field along a and/or b axes. If the internal field lies in the ab plane, the oscillating component in the case of $\mathbf{P}(0) \parallel c$ will be twice as large as that in $\mathbf{P}(0) \perp c$. As H_c (the component of field along c axis) increases, the ratio will decrease from 2 to zero. The nonoscillating component A_{non} , corresponding to roughly 20% of the polarization when $\mathbf{P}(0) \parallel c$, arises from either a nonzero field component parallel to the initial muon spin polarization or an effective zero field at the μ^+ site. To distinguish between these two possibilities in $\mathbf{P}(0) \parallel c$, we applied a weak transverse field (WTF ~ 20 G) on the samples [Fig. 2(a)]. We observed that muons precessed in this field with an amplitude of being roughly equal to A_{non} . This indicates that A_{non} is mainly due to muon sites with local field. There is no contribution in the WTF results from sites with $\mathbf{H}_c \parallel \mathbf{P}(0)$: again, we found that the high internal fields have very small c component. The zero field sites account for approximately 20% of all stopped muons: they may come from either (a) zero internal field at symmetric muon sites in the antiferromagnetic phase or (b) background (such as muons hit on Al behind samples). Since the samples are pure single crystals, it is unlikely that macroscopic regions without static spin ordering exist in the specimen. Below 60 K, from our fits, the relative amplitudes of the two high-frequency signals are approximately equal. Thus the related muon sites corresponding to these signals may be crystallographically symmetrical.

Complementary to neutron scattering, μ^+ SR provides a short-range probe in real space, and is a superb tool for detecting static magnetic order.¹² In ZF- μ^+ SR, the muon precession frequency ν_μ directly reflects the magnetic field distribution at muon sites. In most nonmetallic magnetic systems, the perturbation caused by μ^+ to the magnetism of the host material is known to be minimal. Then we can expect $\nu_\mu(T)$ to follow the sublattice magnetization as $\nu_\mu(T) \propto M_s(T)$ as long as the muon site in the crystal is not altered. In neutron experiments,

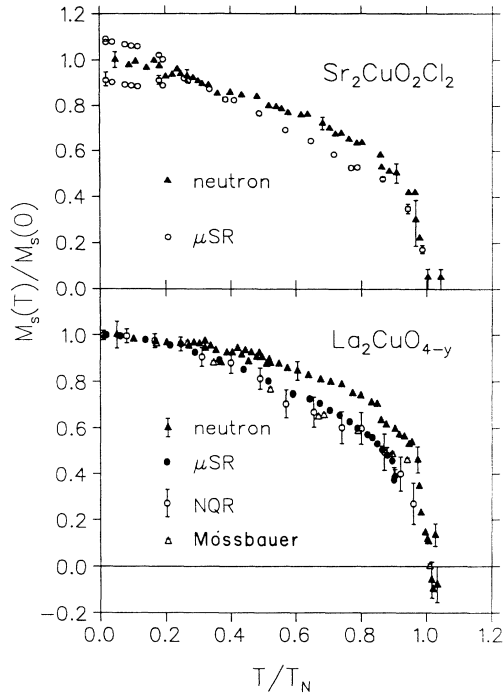


FIG. 6. Reduced sublattice magnetization vs reduced temperature in $\text{Sr}_2\text{CuO}_2\text{Cl}_2$ and La_2CuO_4 .

one measures the intensity of an antiferromagnetic Bragg peak, which is usually proportional to M_s^2 as $I_B(T) \propto M_s^2(T)$. In Fig. 6 we compare the present $\mu^+\text{SR}$ results with neutron studies. We notice that a remarkable difference exists between the curvature of $\nu_\mu(T)$ of $\mu^+\text{SR}$ and $\sqrt{I_B(T)}$ of neutron diffraction. A similar difference was found in La_2CuO_4 . By comparing the La_2CuO_4 data obtained from neutron diffraction,¹³ $\mu^+\text{SR}$,⁷ NQR,¹⁴ as well as Mössbauer effect,¹⁵ we found that the agreement among the latter three techniques is much better than with neutron diffraction (Fig. 6). As discussed in Ref. 6, this difference may be understood as resulting from the sensitive dependence of the Bragg peak intensity I_B on the spatial correlation length of the ordered spins. In addition, neutron results could be subject to the extinction effect. In contrast, μSR or NMR or Mössbauer effect probe the local magnetic field from a few nearby Cu spins as a pointlike probe. In this sense, these three techniques have an advantage over neutron scattering in measuring the temperature dependence of $M_s(T)$.

IV. COMPARISON WITH 2D HEISENBERG MODEL

At low temperature, $M_s(T)$ is mainly reduced by the thermal excitation of magnons. In a quasi-two-dimensional spin Heisenberg system, there is much higher density of states for low energy magnons than in three dimensions. Thus the temperature dependence of $M_s(T)$ should be different from the Brillouin curve for completely three-dimensional systems. The rapid reduction in both ν_μ and $I_B(T)$ at low temperatures in $\text{Sr}_2\text{CuO}_2\text{Cl}_2$ suggest a quasi-two-dimensional magnetic

behavior in this system.

To quantitatively compare the experimental results with theoretical predictions we adopted a quasi-Heisenberg model described by a Hamiltonian:

$$\mathcal{H} = \sum_{NN} JS_u \cdot S_d - \sum_u g\mu_B H_A S_u^z + \sum_d g\mu_B H_A S_d^z, \quad (5)$$

where the subscript u (d) labels spins on “up” (“down”) sites in the ordered phase, the first summation runs over all nearest-neighbor spin pairs, and a small uniaxial anisotropy field H_A stabilizing the magnetically ordered state up to the Néel temperature. (There is no long-range spin order in purely two-dimensional Heisenberg systems.) The solutions by Lines¹⁶ using a random-phase Green’s function approximation for the temperature dependence of the sublattice magnetization show that the reduced magnetization $M_s(T)/M_s(0)$ goes to zero as temperature tends to T_N , and is also affected by the anisotropy $D = g\mu_B H_A / 45J$ normalized to the exchange interaction. As D decreases, the system becomes relatively unstable, which leads to a smaller T_N , and a sharp reduction in $M_s(T)/M_s(0)$. Figure 7 shows the comparison between $\mu^+\text{SR}$ data and results from this model calculation for $S = \frac{1}{2}$. The data are reduced with $\nu_\mu(0) = 16$ MHz, $T_N = 265$ K. We notice that $\mu^+\text{SR}$ data are far different from the molecular field Brillouin curve, and are close to the case of $D \sim 10^{-5}$. This demonstrates that $\text{Sr}_2\text{CuO}_2\text{Cl}_2$ is a two-dimensional magnetic system with very weak anisotropy field. We also notice that for both $\mu^+\text{SR}$ and neutron experiments, the magnetization in $\text{Sr}_2\text{CuO}_2\text{Cl}_2$ is reduced faster than in La_2CuO_4 . This can be qualitatively explained by a smaller anisotropy in $\text{Sr}_2\text{CuO}_2\text{Cl}_2$. In orthorhombic La_2CuO_4 , there is some small effective exchange interaction between the Cu moments on the adjacent CuO_2 planes which defines their relative spin orientations and thus contributes to the anisotropy energy. This is absent in $\text{Sr}_2\text{CuO}_2\text{Cl}_2$ with a tetragonal crystal structure.

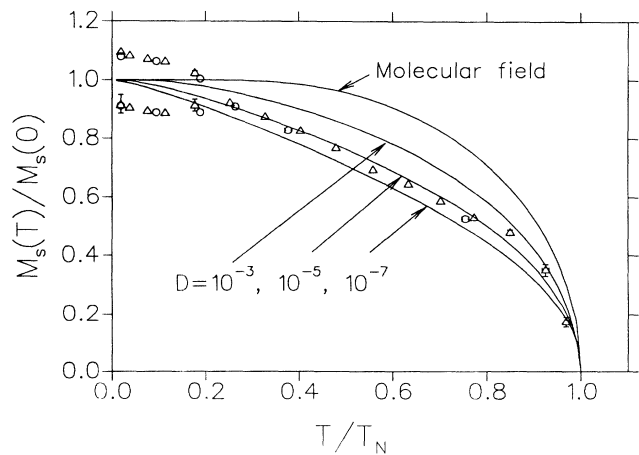


FIG. 7. Comparison M_s derived from ν_μ with 2D Heisenberg model in $\text{Sr}_2\text{CuO}_2\text{Cl}_2$.

V. MUON SITE IN CRYSTAL

The μ^+ SR data have yielded the magnitudes and directions of the internal magnetic fields of $\text{Sr}_2\text{CuO}_2\text{Cl}_2$ at the muon sites as discussed above. In ZF- μ^+ SR the local field is given by,¹⁷ $\mathbf{H}_{\text{loc}} = \mathbf{H}_{\text{dip}} + \mathbf{H}_{\text{hpf}}$, where \mathbf{H}_{dip} is the dipolar field from the Cu^{2+} , and \mathbf{H}_{hpf} is the hyperfine field due to the finite electron spin density at the μ^+ site. Since the hyperfine field is likely to be very small as in the case of La_2CuO_4 , the fields have been calculated from a sum of dipolar contributions:

$$\mathbf{H}_{\text{dip}}(\mathbf{R}_\mu) = \sum_i \frac{-\boldsymbol{\mu} + 3(\boldsymbol{\mu} \cdot \hat{\mathbf{n}}_i) \hat{\mathbf{n}}_i}{|\mathbf{R}_\mu - \mathbf{r}_i|^3}, \quad (6)$$

where $\boldsymbol{\mu}$ is the effective magnetic moment of a Cu^{2+} cation, $\hat{\mathbf{n}}_i$ is the unit vector from the muon to the Cu^{2+} ion at \mathbf{r}_i , and \mathbf{R}_μ is the considered muon site. Because of the r^{-3} dependence, effective contributions to the local field come only from those Cu^{2+} moments in several nearest cells. The fields were evaluated over a radius around 50 Å with average lattice parameters $a = 3.975$ Å, $c = 15.62$ Å. The ordered moment has been measured by neutron diffraction⁴ ($\mu = 0.34 \pm 0.04 \mu_B / \text{Cu}^{2+}$) and magnetic susceptibility⁴ ($\mu \approx 0.6 \mu_B / \text{Cu}^{2+}$). The values are approximately the same as those in La_2CuO_4 (Ref. 12) ($0.5 \sim 0.6 \mu_B$). Therefore we assumed $\mu(T \rightarrow 0\text{K}) = 0.5 \mu_B / \text{Cu}^{2+}$ in our calculation of dipolar fields.

Figure 8 shows the magnetic dipolar field contours on the CuO_2 plane. The field is relatively stable near the center of the plane, but changes rapidly around the oxygen ($H_{\text{O}} = 0$ G) and copper sites. The field lies in the plane, and is of the order of 1 kG. Out of the plane, the field is much smaller (e.g., $H_{\text{Cl}} \approx 170$ G), and becomes zero on the diagonal line: $x + y = 1, z = 0.25$, etc.

The μ^+ probe locations in planar cuprate materials have not received extensive study. It has been suggested that muons may be localized at anion vacancies,^{18,19} or

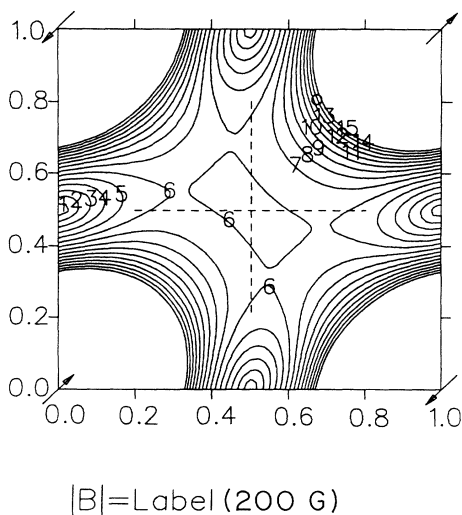


FIG. 8. Contours of dipolar magnetic fields in the CuO_2 plane. The arrows at the corners of the square are the Cu^{2+} spins and oxygen anions are located in the middle of the sides.

other symmetrical sites.^{7,19} Since $\text{Sr}_2\text{CuO}_2\text{Cl}_2$ has a tetragonal structure, and muon sites depend only on the electronic structure, the muon sites should be symmetrically located in a structural unit cell. However, the magnetic field in the cell has lower symmetry [i.e., $H(x, y, z) \neq H(x, 1-y, z)$]. Therefore the single muon rotation frequency implies that the muon sites should be at some symmetrical locations (i.e., $x = 0, \frac{1}{2}$ and/or $y = 0, \frac{1}{2}$). In $\text{Sr}_2\text{CuO}_2\text{Cl}_2$, there is only single frequency above 60 K, and the magnitude and direction of the local field have been determined experimentally. Based on these results, the sites are searched by the restrictions

$$[H(x, y, z) - H(x, 1-y, z)] / H \leq 1\% ,$$

$$H = 1.2 \times (1.0 \pm 0.2) \text{ kG} ,$$

$$H_c / H \leq 20\% .$$

This leads to three possible muon locations near (a) the dashed cross in the center of the CuO_2 plane ($d_{\mu-\text{O}} \geq 0.8$ Å, Fig. 8); (b) on the line between Cu^{2+} and apical Cl^- with a distance of $d_{\mu-\text{Cl}} \approx 1.2$ Å to Cl site, (c) on the side of CuO_2 plane with a distance of $d_{\mu-\text{O}} \approx 0.35$ Å to oxygen site. Case (c) is unlikely, since the distance between μ^+ and the nearest oxygen in this case is much smaller than the μ -O bond length of about 1 Å.²⁰⁻²²

At low temperatures there are two muon precession frequencies. From previous discussions, the frequency splitting may be due to spin reorientation. However, we fail to find the splitting in both cases (a) and (b), except for the unlikely case with the coexistence of two inequivalent domains with different spin structures. At the moment, it is not possible to develop a successful model for the frequency split below 60 K if we assume the above-mentioned high-symmetry sites (a) and (b) and spin reorientation. Multiple muon spin precession frequencies at low temperatures have been observed in several other insulator magnetic systems, such as $\alpha\text{-Fe}_2\text{O}_3$ (Ref. 21) or YFeO_3 .²² The frequency splits in these materials were ascribed to metastable muon sites^{21,23} and/or to change of muon sites in the different temperature regions. It is also possible to consider muon sites with lower symmetry in the CuO_2 plane other than (a) and (b). For example, if the muon site is on the diagonal line in the CuO_2 plane, there are two muon precession frequencies. Above 60 K, the muon site may be changed to some higher symmetric sites like (a) and (b): resulting in only one frequency. Such a muon site change could provide alternative way of explaining the frequency split at low temperatures.

The internal field at the muon sites in $\text{Sr}_2\text{CuO}_2\text{Cl}_2$ (1.2 kG) is much higher than those in La_2CuO_4 (400 G) and Nd_2CuO_4 (300 and 140 G). Since the crystal structures and the ordered moments in these systems are similar, the difference must be due to different μ^+ sites. By applying similar consideration to La_2CuO_4 and Nd_2CuO_4 , we find the muon sites in both systems are near the planes containing the out-of-plane oxygens or apex oxygens, and are more likely close to these oxygens to form μ -O bond. The difference in the muon sites can be explained by the replacement of the apex O^{2-} by Cl^- in

$\text{Sr}_2\text{CuO}_2\text{Cl}_2$. Because of the reduced ionic charge of Cl^- , the site near the apex Cl is no longer as attractive to the μ^+ as that near O^{2-} in terms of the electrostatic energy. Then it seems reasonable that the predominant muon sites move to the CuO_2 plane containing the O^{2-} ions.

VI. CONCLUSION

Magnetic order in single crystals $\text{Sr}_2\text{CuO}_2\text{Cl}_2$ was observed in the ZF- μ^+ SR experiment below $T_N \approx 260$ K. The temperature dependence of the muon precession frequency exhibits properties characteristic to the two-dimensional spin- $\frac{1}{2}$ magnetic system with a dominant Heisenberg interaction and very small anisotropy. The smaller anisotropy in this system than that in La_2CuO_4 is consistent with the tetragonal structure of $\text{Sr}_2\text{CuO}_2\text{Cl}_2$. The substitution of Cl for the apex oxygens leads to some different features than those in La_2CuO_4 , such as larger c -axis parameter, smaller Madelung potential at copper site for introducing an electron, and different muon sites. The comparison of muon sites among $\text{Sr}_2\text{CuO}_2\text{Cl}_2$, La_2CuO_4 , and Nd_2CuO_4 suggests a possible evidence that

muon sites are closely associated with the oxygen atoms in the oxide superconductors.⁹ The splitting of ν_μ observed at low temperature indicates either the existence of spin reorientation or changing of the muon sites. Further works by polarized neutron scattering can test the assumption of spin reorientation.

ACKNOWLEDGMENTS

The authors thank A. S. Arrott, V. J. Emery, and G. Shirane for helpful discussions, and C. Ballard and K. Hoyle of TRIUMF for technical support. Work at Columbia University was supported by the National Science Foundation under Contract No. DMR-89-13784 and by the David and Lucile Packard Foundation and at TRIUMF by a Grant from the Natural Sciences and Engineering Research Council (Canada) and National Research Council of Canada. Ames Laboratory is operated for the U.S. Department of Energy by Iowa State University under Contract No. W-7405-Eng-82. Work at Ames was supported by the Director for Energy Research, Office of Basic Energy Sciences.

¹G. J. Bednorz and K. A. Müller, *Z. Phys. B* **64**, 189 (1986).

²B. Grande and Hk. Müller-Buschbaum, *Z. Anorg. Allg. Chem.* **417**, 68 (1975).

³L. L. Miller *et al.*, *Phys. Rev. B* **41**, 1921 (1990).

⁴D. Vaknin *et al.*, *Phys. Rev. B* **41**, 1926 (1990); (unpublished).

⁵Madelung potentials at copper sites for hole doping can be found in J. B. Torrance and R. M. Metzger, *Phys. Rev. Lett.* **63**, 1515 (1989).

⁶D. C. Johnston *et al.*, *Phys. Rev. B* **36**, 4007 (1987), and references therein; D. C. Johnston *et al.*, *Physica C* **153-155**, 572 (1988); D. Vaknin, *et al.*, *Phys. Rev. Lett.* **58**, 2802 (1987); S. Mitsuda *et al.*, *Phys. Rev. B* **36**, 822 (1987); T. Freltoft *et al.*, *ibid.* **36**, 826 (1987); T. Freltoft *et al.*, *ibid.* **37**, 137 (1988); S. K. Sinha *et al.*, *J. Appl. Phys.* **63**, 4015 (1988).

⁷Y. J. Uemura *et al.*, *Phys. Rev. Lett.* **59**, 1045 (1987); *Physica C* **153-155**, 769 (1988).

⁸Y. Endoh *et al.*, *Phys. Rev. B* **40**, 7023 (1989); J. Akimitsu *et al.*, *J. Phys. Soc. Jpn.* **58**, 2646 (1989).

⁹G. M. Luke *et al.*, *Physica C* **162-164**, 825 (1989); (unpublished).

¹⁰R. S. Hayano *et al.*, *Phys. Rev. B* **20**, 850 (1979); Y. J. Uemura *et al.*, *ibid.* **31**, 546 (1985); A. Schenck, *Muon Spin Rotation*

Spectroscopy: Principles and Applications in Solid State Physics (Hilger, Bristol, 1986).

¹¹This could be due to muon diffusion as well, which has been observed in some other high- T_c systems above 250 K.

¹²Y. J. Uemura *et al.*, *Hyp. Int.* **49**, 205 (1989).

¹³K. Yamada *et al.*, *Solid State Commun.* **64**, 753 (1987).

¹⁴H. Nishihara *et al.*, *J. Phys. Soc. Jpn.* **56**, 4559 (1987).

¹⁵S. Jha *et al.*, *Hyp. Int.* **50**, 607 (1989).

¹⁶M. E. Lines, *J. Phys. Chem. Solid* **31**, 101 (1970).

¹⁷A. B. Denison *et al.*, *Helv. Phys. Acta* **52**, 460 (1979).

¹⁸F. H. Gygax *et al.*, *Europhys.* **4**, 473 (1987); J. W. Schneider *et al.*, *Phys. Lett. A* **124**, 107 (1987); F. N. Gygax *et al.*, *ibid.* **127**, 447 (1988); C. Bucci *et al.*, *ibid.* **127**, 115 (1988).

¹⁹J. I. Budnick *et al.*, *Phys. Lett. A* **124**, 103 (1987); A. Golnik *et al.*, *ibid.* **125**, 71 (1987).

²⁰C. Boekema, *Hyp. Int.* **8**, 609 (1981); W. K. Dawson *et al.*, *J. Appl. Phys.* **64**, 5809 (1988).

²¹C. Boekema *et al.*, *J. Magn. Magn. Mater.* **36**, 111 (1983); *Hyp. Int.* **17**, 305 (1984).

²²E. Holzschuh *et al.*, *Phys. Rev. B* **27**, 5294 (1983).

²³A. Browne and A. M. Stoneham, *J. Phys. C* **15**, 2709 (1982).